Title: An investigation into metal organic cage's effectiveness in transporting selected diazo compounds through a liquid membrane.

Research question: How does the type of geometric isomerism (cis or trans isomerism) of an organic Diazo-compound affect the thermodynamics and chemical kinetics of its transport through a liquid membrane containing a $Fe^{II}_4L_6$ metal-organic cage.

Research Author: Usman Kashif
Research Mentor: Jiratheep Pruchyathamkorn

Abstract:

Chemical filtrations and separations require up to 15% of the global energy budget. At the same time, the combustion of hydrocarbon fuels accounts for 73% of total U.S Green House Gas Emissions. Metal organic cages (MOCs), constructed from hydrocarbon linkers and metal ions, and able to encapsulate and release targeted molecules based on geometric orientation. Thus, MOCs can be used as a technological tool used for molecular separation. In this paper, aqueous solutions of a $Fe^{II}_4L_6$ metal-organic cage were used as liquid membranes to facilitate the transport of two isomers of the same diazo-compound. Solved differential equations were used as kinetic models for the relationship between the concentration of each isomers through the liquid membrane. The concentration of each diazo isomer was monitored using NMR spectroscopy in the feedstock and receiving arm of the U-tube membrane. Fitting the kinetic models to the monitored concentrations and using the *Excel* solver procedure yielded the parameters for the rate of guest-encapsulation (k_f) and guest-release (k_r) for each isomer. Then by using a guest-binding equilibrium model, the equilibrium constants (K_{eq}) for both systems were determined. The change in Gibbs Free energy (ΔG) was also determined for the system with each isomer and provide insight about the more spontaneous and thermodynamically favored/stable system. The results concluded that the *trans*-isomer transported at a faster rate (k_f = 0.150 and k_r = 0.120) than the *cis*-isomer (k_f = 0.0574 and k_r = 0.0600). However, the cis isomer demonstrated greater thermodynamic stability in the MOC. The higher K_{eq} and lower ΔG value for the *cis*-isomer system (K_{eq}= 1.05 and ΔG = -120) as compared to the *trans*-isomer system (K_{eq}=0.800 and ΔG = -1200 show that the *cis*-isomer system is more thermodynamically favorable and spontaneous with a higher energy barrier at the guest-uptake and guest-release phase boundaries.

Introduction:

Metal-Organic cages (MOCs) are crystalline materials that are constructed from inorganic metal ions and organic linkers. This structure forms a cage-like shape with empty cavities. MOCs are different from other porous materials due their unique structural diversity. They have porous structures, precise atomic arrangement, and interconnected ligands with rotatable bonds. Amongst the vast applications of MOCs, they have been recently used as a tool for molecular separation. The metal organic cage used as a separation tool in this paper is a coordination

cage, formed by the spontaneous organization of metal ions and organic ligands. These metal-organic structures are formed by the reversable ligand metal dative bond in which an organic ligand donates its lone pair of electrons to the central metal ion. The metal ions are coordinated to many ligands and create polyhedral nodes. These can have several molecular shapes due to the nature of the central ion and coordination environment. Metal organic cages are used for molecular separation due to their selective permeability function. These cage macromolecules contain empty nanocavities with open windows that allow molecules to enter and bypass. MOCs can be used for molecular separation based on size and the affinity for the cage's interior. The aqueous membrane used in this separation process consists of an immiscible fluid phase that separates two other liquids. Coordination cages are used in the aqueous membrane as active carriers and hosts of selected molecules. (1)

The molecular separation process using MOCs during the transport of a selected compound through the liquid membrane occurs in three stages: guest intake in the feedstock arm, transport in cage within aqueous membrane, and guest release in the receiving phase. For this investigation, the selected compound transported through a U-tube liquid membrane with the feedstock and receiving arms on each side of the tube with the aqueous transport membrane in the U-shaped section. The guest intake refers to the process by which the selected molecule encapsulates itself into the MOC, and is dependent on molecular size, orientation, and stoichiometry of addition. Hydrogen bonding, London dispersions, π-π stacking, among other non-covalent interactions are the forces behind guest encapsulation. Coordination cages are used as liquid – phase extractants to encapsulate target molecules from an immiscible liquid phase. They are classified as liquid – phase extractants as they bring in the guest molecules (organic solvents) into solvents that they are not typically soluble in. The separated molecules not entrapped in the cage remain on the feedstock side of the membrane. Initially, the concentration of guest-molecule in feedstock arm before cage-binding is higher, and as the guest molecule encapsulates into the MOC, their concentration in the feedstock phase gradually decreases.

The encapsulated guest molecules are stabilized in the cages due to the hydrophobic interactions in the guest-binding process. The hydrophobic contribution is the attraction between the targeted molecules and the hydrophobic interior of the MOC. This phenomenon causes the initial binding, but the salvation effect of the guest molecules being surrounded by water molecules stabilizes the new guest-MOC complex. The guest molecule is then transported through the aqueous membrane. The chemical kinetics of the cage-guest transport in the aqueous membrane depends heavily on guest binding affinity. This affinity refers to the strength of the attraction between the encapsulated guest molecules and the MOC. Thus, the rate at which these guest molecules are transported through the U-tube is influenced by the binding affinity in the cage. In general, guest molecules that are more hydrophobic in nature and smaller in size tend to have a higher binding affinity and thus transport at a faster rate. Another factor that influences the rate of transport is the concentration gradient – the difference in concentration of the guest molecule between the guest-intake and guest-release process. The concentration gradient impacts the diffusion coefficient of the guest molecule. The diffusion

coefficient measures how freely and easily the guest molecule can move within the liquid membrane during transit in the MOC. A steeper concentration gradient corresponds to a higher diffusion gradient and this an increase in the rate of guest transport across the U-tube.

The guest-release stage of the transfer occurs in the receiving phase boundary of the system. Similar to the guest intake process, the guest release is influenced by the cage-guest molecule binding affinity. A higher binding affinity results in a slower rate of release. The sudden release of these guest molecules from their entrapment in the MOC can be triggered from external stimuli, competitive binding, equilibrium shift, and kinetic factors. External stimuli like fluctuation in pH and light can trigger guest-release from the MOC. For example, inducing exposure of light of a specific wavelength in the receiving phase boundary can create conformational changes within the MOC and a consequential guest-release. Alternatively, the presence of other molecules in the receiving end with a greater binding affinity to the cages can cause the displacement of the existing guest molecule. A rise in the concentration of the guest molecule at the receiving arm may cause an equilibrium shift and thus guest release. According to Le Chatelier's Principle, a system at equilibrium will counteract any change by shifting the equilibrium. As the guest concentration increases, the equilibrium will shift to the side of the reaction that reduces the guest concentration – guest release. The binding, transport in MOC, and guest – release occur under specific conditions of dynamic equilibrium and are influenced by kinetic factors such as the k_f (rate constant in feedstock arm) and k_r (rate constant in receiving arm). (2)

Reviewing previous literature: The use of a MOC for molecular separation and guest molecule transport through a liquid membrane has been explored in depth by Bao-Nguyen T. Nguyen and team at the University of Cambridge in 2021. The study concentrated on the ability of coordination cages to selectively transport Naphthalene (dissolved in dodecane) across a liquid membrane with metal organic cages. Naphthalene's high binding affinity to the cages used in the investigation made it suitable for the guest molecule. The metal organic cages used in this paper were comprised of sulfate salts $Fe^{II}_4L_6$ (cage 1) and $Co^{II}_4L_4$ (cage 2), both tetrahedral in molecular geometry. Each cage was prepared and dissolved in water. The aqueous solution of both cages flowed into the U-tube section (stock arm) of the U-tube system. Feedstock solutions of naphthalene were loaded into the feedstock arm of each U-tube (one for each cage). Each cage successfully employed selective permeability to encapsulate the guest naphthalene molecule and transport it across the aqueous membrane. A three-state model was used to approximate the concentration of the guest naphthalene through the guest-intake (N_A), transport (N_b), and guest release (N_c). In this investigation, the value of N_b was not directly measured but derived from mass balance.

$$N_A \underset{T_r}{\overset{T_f}{\rightleftharpoons}} N_B \underset{T_f}{\overset{T_r}{\rightleftharpoons}} N_C$$

Where T_f is the forward transport constant and T_r is the reverse transport constant. The results show that the time taken for 50% of the naphthalene from the feedstock to the receiving arm is 1.99 days for the aqueous membrane with the $Fe^{II}_4L_6$ cages, while a relatively larger duration of 9.41 days for the liquid membrane containing $Co^{II}_4L_4$ cages. Bao-Nguyen T. Nguyen and team attributed the longer transport time in the latter cage due to its more enclosed framework and higher activation energy barrier for guest intake and release. In the first cage, the uptake and release movements of the guest molecule occurred at faster rates due to the stronger hydrogen bonds between the flexible glycerin chains that govern the opening and closing of the apertures in the MOC. This cage consisted of a more framework with apertures more suitable for the intake and release of naphthalene molecules. To investigate the chemical kinetics of the system, the concentration vs time data for N_A and N_c were fit simultaneously through a non-linear least squares fir for the data using Mathematica software. The resulting best fit equation suggested a first order rate constant for naphthalene transfer from the dodecane solution into the MOC (k_f^{obs}) and for the reverse reaction for naphthalene to dodecane (k_r^{obs}). The forward (T_f) and reverse (T_r) transfer constants were calculated by dividing the observed rate constants k_f^{obs} and k_r^{obs} by the cross-sectional area of the U-tube (1.13 cm^2) and by the cage concentration (2.0 mM) respectively. The team then calculated and compared the molar fluxes for the transport of naphthalene our of and into the organic solvent. The molar flux for the transport of naphthalene into each of the metal-organic cages can be determined using the following rate law:

$$J_f = T_f[N]\left[cage\right] \quad \text{(Equation 1)}$$

where J is the molar flux and N is the concentration of naphthalene in either arm of the U-tube. Similarly, the molar flux for the transport of naphthalene out of the MOC and into the dodecane solution can be determined using the following rate law:

$$J_r = T_r\left[N_B\right] \quad \text{(Equation 2)}$$

Another parameter calculated was K_{eq}, calculated by dividing T_f by T_r, which represents naphthalene's preference to be encapsulated by the MOC to be dissolved in the organic solved. A $K_{eq} > 1$ signifies a preference for being sequestered while a $K_{eq} < 1$ represents a preference for being dissolved. After modelling using Mathematica software and applying the calculations, all relevant parameters were found. The T_f for cage 1, rate constant for $Fe^{II}_4L_6$ cage binding, was found to be 0.157 $mM^{-1}day^{-1}cm^{-2}$, while the T_r for cage 1, rate constant for guest-release, was found to be 12 $day^{-1}cm^{-2}$. The T_f for cage, rate constant for $Co^{II}_4L_4$ cage binding, was found to be 0.045 $mM^{-1}day^{-1}cm^{-2}$, while the T_r for cage 2, rate constant for guest-release, was found to be 0.13 $day^{-1}cm^{-2}$. The researchers also observed that when the second MOC was used for naphthalene transfer, there was a slight sigmoidal rise in the concentration of naphthalene in the receiving arm. This rise in concentration indicates an induction period, or a delay in the guest-transfer attributed to the build-up of a host-guest intermediate within the cage layer. This delay was only observed when using the $Co^{II}_4L_4$ cage. (3)

The recorded kinetic data showed that the molar flux for naphthalene release back into the organic solvent was higher than the molar flux for the naphthalene – cage binding for both cages. This is consistent with the K_{eq} values of 0.013 and 0.32 for cage 1 and cage 2 respectively. In both cases, the naphthalene prefers to be dissolved in the organic solvent of dodecane than be bound to the MOC. The higher T_f and T_r values for the cargo of Naphthalene in cage 1 suggests faster overall guest intake, transport, and release. The researchers attributed this to the cage structure and stronger molecular binding affinities as aforementioned.

The existing literature for the use of metal organic cages for molecular separation in a liquid membrane, specifically the study of the transport of Naphthalene by Bao-Nguyen T. Nguyen and team, demonstrate the underlying chemical kinetic principles that govern the transfer of selected compounds through an aqueous membrane containing MOCs. This paper will apply the same three state model to demonstrate the underlying chemical kinetics and thermodynamics of the transfer of two isomers of the same diazo-organic compound through a liquid membrane consisting of the same $Fe^{II}_4L_6$ and $Co^{II}_4L_4$ metal organic cages.

Diazo-compounds are a special type of organic compounds that contain a characteristic diazo-group. All diazo compounds have two linked nitrogen atoms that are double bonded (N=N) at the terminal position of the organic compound. These compounds follow the general structure form of R=N=N-R, where R signifies a hydrogen atom or other functional group. Diazo compounds have an electronic structure consisting of delocalized pi electron density over the α-carbon and two nitrogen atom. The structure also has an orthogonal π system with electron density delocalized over only the terminal nitrogen atoms. In this investigation, the concentration of two isomers of the same halogenated diazo compound was monitored as it transferred through the liquid membrane. The structure of a halogenated diazo compound is illustrated below.

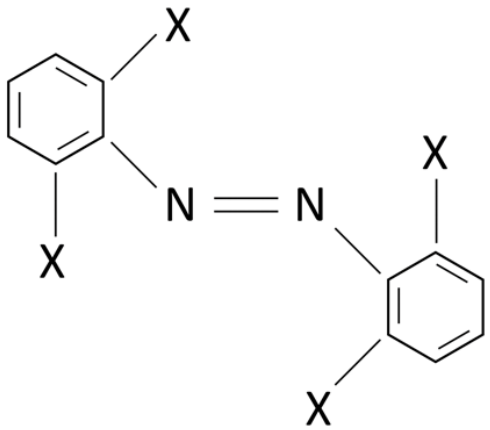

The diazo compound exhibits cis-trans isomerism, which arises due to the restricted rotation around the double bond (N=N). This restricted rotation can lead to different spatial arrangements of the substituents around the diazo functional group and the attached halogen atom. The position of the substituents and halogen atom around the diazo group give the molecule two distinct isomers.

In the *cis*-isomer of the R=N=N-R diazo structure , both the “R” groups are found on the same side of the diazo-group. In the *trans*-isomer, the the R groups are located on opposite sides of the diazo compound. The cis isomer has a bent shape with a net dipole moment due to the both the R groups being placed on the same side of the molecule. The opposite arrangement for the trans isomer allows for a linear shape with a lower boiling point due to no dipole moment. The differing geometric orientation of the cis and trans isomers of the diazo compounds impact their physical properties, stability, and reactivity in chemical processes. Changes in such parameters due to the isomerism of the diazo-compound impacts both its rate of transport through the MOC as well as the diazo-cage binded thermodynamic stability.

The metal organic cage used for selective transport of both isomers was the same $Fe^{II}_4L_6$ cage as used in Bao-Nguyen T. Nguyen’s study. The shape and structure of this cage has vast impacts on the selected transport of the diazo isomers. The $Fe^{II}_4L_6$ cage is formed through the coordinate covalent bonds between the aromatic organic ligands and iron ions. The cage follows a tetrahedral arrangement with four iron ions at the vertices of the tetrahedron. These ions are attracted to six organic ligands to form the cage structure. The cage has an internal cavity lined with organic ligands, which provides a hydrophobic environment for diazo molecule transport. The coordinate bond formed between the iron ions and the organic ligand give a stable coordination complex structure for the MOC. This cage is also known as tetrazine-edged $Fe^{II}_4L_6$ tetrahedra, where the tetrazine edges refer to the organic ligands. The aromatic core of the organic ligands contains a tetrazine ring, which contains one carbon atom and four nitrogen atoms. These tetrazine edges provide a rigid and planar structure for the guest binding molecules to enter into. The tetrazine-edged $Fe^{II}_4L_6$ tetrahedra can also undergo structural modification when the guest binding process occurs. Structural transformation of the metal organic cage once the diazo-compound has binded are triggered from the inverse electron-demand Diels-Alder (IEDDA) reactions. These IEDDA reactions occur between a strained dienophile (electron-deficient) and a diene (electron-rich) to form a cycloadduct. In context, the tetrazine edges are the strained dienophile and the diazo compound serve as the diene. When these react, the cage undergoes post assembly modification that introduce new functionalities. These new functionalities can alter the shape, size, and binding properties and reactivity of the MOC. (4)

The different geometric orientations of each diazo isomer can result in different structural modifications of the cage and thus differing rates of guest-uptake and guest-release as well as varying thermodynamic stability. In order to measure the aforementioned parameters, NMR spectroscopy was employed to independently measure the concentration of the guest diazo isomers in the feedstock and receiving arm of the U-tube. Then, modelling the concentration

versus time of the diazo-compound through the liquid membrane using solved differential equations can yield the required rate of guest-uptake and guest-release parameters.

For scientific simplicity, this procedure assumes that the concentration of metal organic cage does not change throughout the transport process. The cage concentration before guest-binding, within the transport section of the U-tube, and after guest-release is assumed to remain constant.

Results:

The relationship between the rate of change of the concentration of these diazo-compounds through the three stages of the liquid membrane U-tube can be modelled using the following differential equations:

Through feedstock arm: $\frac{dN_A}{dt} = -k_f N_A(t) + k_r N_B(t)$ (Equation 3)

Through U-section (transfer in MOC): $\frac{dN_b}{dt} = +k_f N_A(t) - 2k_r N_B(t) + k_f N_C(t)$ (Equation 4)

Through receiving arm: $\frac{dN_C}{dt} = +k_r N_B(t) - k_f N_C(t)$ (Equation 5)

To determine a model for the concentration of the diazo compound through the liquid membrane in each of the three stages of transport, the equations above can be integrated using the appropriate boundary conditions ($N_A = N_{A0}$, $N_B = N_{B0}$, and $N_C = 0$). These boundary conditions assume that the diazo compound is in only the feedstock arm at t=0. The solutions to the differential equations are shown below.

$$N_A = \frac{(k_f(1+e^{-2k_r t}))+2k_r(1+e^{k_f t}))e^{-k_f t}}{2(k_f+2k_r)} N_{A0} \quad \text{(Equation 6)}$$

$$N_A = \frac{k_f(1-e^{-(k_f+2k_r)t}))}{k_f+2k_r} N_{A0} \quad \text{(Equation 7)}$$

$$N_C = \frac{(-k_f(1-e^{-2k_r t})) - 2k_r(1-e^{k_f t}))e^{-k_f t}}{2(k_f+2k_r)} N_{A0} \quad \text{(Equation 8)}$$

The above equations can now be used to determine the value of for both diazo-compound transfer from the solution into the MOC (k_f) and for the reverse reaction for diazo-compound to solution (k_r). By independently measuring the time vs concentration of N_A and N_c through NMR spectroscopy, the solver procedure on *Excel* for non-linear fitting can be used to determine k_f and k_r values for guest-uptake and guest release of the diazo-compounds. (5)

Raw data table: Relationship between the concentration of both isomers of organic diazo-compound in the feedstock arm (N_A) and the receiving arm (N_C) of the U-tube in the liquid membrane.

Compound 1: *Cis*-isomer

Time (Hour)	N_A	Nc
0	10.00	0.00
1	8.90	0.07
3	7.48	0.49
6	6.10	1.23
9	5.31	1.91
11	4.90	2.26
15	4.42	2.75
18	4.16	3.00
21	3.98	3.18
24	3.88	3.29
27	3.77	3.38
30	3.72	3.44
33	3.67	3.48
36	3.54	3.51
39	3.63	3.53

Compound 2 – *Trans*-isomer

Time (Hour)	N_A	Nc
0	10.00	0.00
1	9.45	0.02
3	8.51	0.12
6	7.31	0.40
9	6.56	0.73
11	6.15	0.95
15	5.45	1.38
18	5.01	1.66
21	4.75	1.91
24	4.46	2.12
27	4.31	2.31
30	4.12	2.46
33	3.98	2.60
36	3.87	2.71
39	3.77	2.80

The above raw data have been best-fit modelled into the parent equation from equation 4 and equation 6 for each diazo-compound isomer in each arm of the U-tube.

The plot of the best-fit concentration versus time and the modelled k_f and k_r values are shown below.
Processed Data: Scatter plots visually representing the concentration changes of both isomers of the organic diazo compound through the feedstock and receiving arm at each hour of selected transport using the metal organic cage.

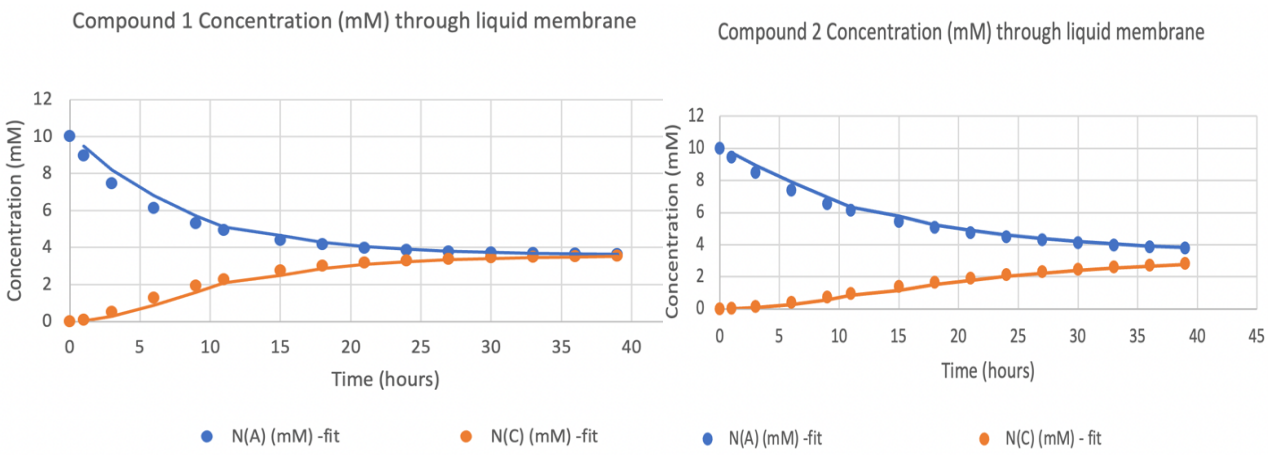

The *Excel* solver procedure non-linear fitting computes the required k_f and k_r values as summarized in the table below. Note the use of moving average fit for the line of best fit for the data instead of an exact curve– this is a limitation of the Excel modelling software.

Table 1: Rate constants for the transport of cis and trans isomer of diazo compound through aqueous layer containing metal organic cage.

	k_f (rate of guest-uptake (day^{-1}))	**k_r (rate of guest-release (day^{-1}))**
***Trans*-isomer**	0.150	0.120
***Cis*-isomer**	0.0574	0.0600

Results Analysis and Discussion:

Table 1 demonstrates how the rate of transport into the cage for the *trans*-isomer is greater than that of the *cis*-isomer (0.150>0.0574) and the rate of release back into the liquid membrane for the *cis*-isomer is also greater than that of the *trans*-isomer (0.120>0.0600). These parameters indicate that the overall guest-uptake and guest-release process occurs faster for the transport of the *trans*-isomer of the diazo compound than that of the *cis*-isomer inside of the liquid membrane. Although these rates of transport processes suggest a faster transport for the *trans*-isomer, they do not explain the thermodynamic stability and guest-binding affinities of the respective isomers. (6)

The stability of the guest Diazo-compound within the metal organic cage can be furthered analyzed through the calculation of the equilibrium constant during the guest-binding and guest release process, K_{eq}. By definition $K_{eq} = \frac{N_B}{N_A}$ (ratio of concentration of Diazo-compound after transport process to concentration prior guest-binding process).

At equilibrium, the rate of transport of the Diazo-compound into the cage (with initial concentration N_A and rate constant k_f) is equal to the rate of Diazo-compound release back into the liquid membrane (with guest-cage binded concentration N_B and rate constant k_r).

$$\text{Rate of guest intake} = k_f \left[N_A\right] \quad \text{(Equation 9)}$$

$$\text{Rate of guest release} = k_r \left[N_B\right] \quad \text{(Equation 10)}$$

$$\text{At equilibrium } k_f \left[N_A\right] = k_r \left[N_B\right] \quad \text{(Equation 11)}$$

$$\text{Rearranging yields: } \frac{k_f}{k_r} = \frac{\left[N_B\right]}{\left[N_A\right]} = K_{eq} \quad \text{(Equation 12)}$$

The value of K_{eq} has been calculated for both isomers using the ratio $\frac{k_f}{k_r}$ and recorded in the table below:

	***Trans*-isomer**	***Cis*-isomer**
K_{eq}	0.800	1.05

A higher K_{eq} value indicates a greater concentration of the Diazo-compound after the guest-binding process than before the process at the equilibrium. This means that a higher K_{eq} value suggests that the system in the liquid membrane found the binding process more thermodynamically favorable, leading to the formation of more products (diazo-MOC binded complex) compared to the reactants (free diazo compound). Thus, the *cis*-isomer with the higher K_{eq} (1.05) compared to the *trans*-isomer (0.800) indicates that the diazo-compound is more thermodynamically stable post MOC-binding process as compared to the *trans*-isomer. (7)

Discussion:

Thus, the obtained results demonstrate that the rate of transport at both phase boundaries (guest-uptake in the feedstock arm and guest-release in the receiving arm) is faster for the trans isomer than for the cis isomer. However, the K_{eq} values suggest that the MOC-binding process is more thermodynamically favorable for the cis isomer than the trans isomer. These unexpected results can be explained by the fact that the higher thermodynamic stability of the cage-binded cis diazo compound required more time to reach due to the high energy barrier involved in the binding process.

The higher energy barrier of the *cis*-isomer binding and release process may be attributed to its geometric orientation, high boiling point, and reactivity. In relation to boiling point, the cis

isomer's higher boiling point means an increased molecular viscosity. The higher viscosity of the diazo compound slows down its diffusion through the liquid membrane and results in a slower binding and release process from the MOC. This is evidenced by the slower rate of guest-uptake (0.0574 day^{-1}) and guest-release (0.0600 day^{-1}) for the *cis*-isomer. The more viscous the diazo compound, the more resistant it is to flow in the aqueous membrane and longer it takes for the binding to the cage, hence the slower rate of transport. The bent shape and net dipole moment for the *cis*-isomer may cause stronger binding to the MOC, as evidenced by the higher K_{eq} (1.05) value, yet still require a higher energy barrier to overcome in the guest-binding process. Stronger intermolecular forces require more energy to overcome, especially at the guest-encapsulation and guest-release phases of the MOC. The higher energy barrier required to establish new binding interactions between the Diazo compound and the MOC may result in a slower yet stronger binding process. (8)

The geometric orientation of the cis isomer also plays a role in the higher energy barrier for transport. The substituents in the cis isomer are arranged on the same side of the molecule, and this results in increased steric hindrance and hindered diffusion. The position of the bulky substituents in the cis isomer may result in their clashed interactions with other molecules in the membrane as well as the organic ligands in the MOC. This causes steric hindrance – the congestion caused because of the physical presence of surrounding ligands which impedes binding interactions and molecular movement. The bent shape of the cis isomer results in an increased steric hindrance, whereas the linear shape of the *trans*-isomer does not result in the same effect. The substituents in the trans isomer of the diazo compound are arranged in a straight line, which allows for easier binding and movement. This linear arrangement minimizes steric interactions and facilitates faster transport into and out of the MOC. This supports the data showing the higher k_f and k_f values for the trans isomer as compared to the cis isomer. (9)

The thermodynamic stability of the guest molecule during guest-binding, encapsulation, and guest-release can also be determined using a calculation of the Gibbs Free Energy (G). The G value measures the maximum amount of work done in a system under constant temperature and pressure conditions. The change in Gibbs Free Energy (ΔG) measures the spontaneity of a reaction. If ΔG <0, then the reaction is spontaneous and thermodynamically favorable. The more negative the ΔG value, the greater the tendency for the system to move toward the equilibrium and achieve thermodynamic stability. ΔG can be calculated using the following equation:

$$\Delta G = -RTlnK_{eq}$$

(Equation 13)

In equation 13, R is the gas constant = 8.31, T represents temperature, and K_{eq} is the equilibrium constant during the transport in the MOC. The system temperature at which the concentration of each diazo compound was monitored as it transferred through the liquid membrane was set at the standard room temperature of 25°C or 298 K. (10)

The ΔG values for the system of each isomer of the diazo compound has been calculated using equation 8. The obtained parameters are shown in the table below.

	***Trans*-isomer**	***Cis*-isomer**
ΔG	552	-120

The calculated ΔG value of the system during *trans*-isomer transport of 552 indicates a non-spontaneous and thermodynamically unstable system. In contrast, the calculated ΔG value of the system during *Cis*-isomer transport of -120 indicates spontaneity and greater thermodynamically stability. This result is consistent with the calculations of the rate of guest uptake and release as well as the determined K_{eq} values. Within the metal organic cage, a more thermodynamically stable compound will be less resistant to decomposition. Thus, in relation to Gibbs free energy, a positive value of ΔG = 552 suggests that between guest encapsulation and guest release the *trans*-isomer diazo compound may have decomposed due to less product stability as compared to the *cis*-isomer. (11)

Methods and Evaluation:

The results obtained have been analyzed through both a thermodynamics and chemical kinetics lens. All the calculated parameters, obtained from the Excel procedure fitting data to the kinetic model, demonstrate that the rate of transport (including MOC encapsulation and release) is faster for the *trans*-isomer than the *cis*-isomer due to its more convenient geometric orientation. However, the *cis*-isomer has greater stability inside of the MOC as compared to the *trans*-isomer, primarily due to the higher energy barrier in the guest-cage binding process and greater spontaneity as seen by the ΔG value.

A limitation to the three-state model used for approximating concentration throughout the membrane is that it assumed constant cage concentration. This simplification is known as steady state approximation, a common tool used in chemical kinetics to simplify the analysis of reactions including intermediates or other reactants and products formed within the U-tube liquid membrane. The steady state approximation was employed to assume the $Fe^{II}_4L_6$ cage concentration to be constant throughout encapsulation, transport, and release. In addition, the simplified three-state model used to derive the kinetic equations employed the steady state approximation to simplify the kinetic expression for product concentration. By assuming that the concentration of the intermediate remains constant, the steady state approximation allows for the derivation of a simplified rate law from the many elementary steps. (12)

A more accurate model for the guest concentration through the membrane would take into consideration the cage with its own. However, a rate expression that includes the concentration of the cage species would yield a second order differential equation to model the rate of change of the concentration of the diazo compound through the three stages of the liquid membrane.

The Excel solver procedure is not suitable for second order models and thus the values of k_f and k_r would not be obtained. Thus, for the sake of simplicity, the three-state model - and thus a first order rate expression – was used to yield the required k_f and k_r values.

Conclusion:

Overall, this paper has outlined the use of a $Fe^{II}_4L_6$ metal organic cage for selected transport of a guest Diazo compound through a liquid membrane and used kinetic models to analyze the differences in the kinetics and thermodynamics of the system when two different diazo isomers were transported. Understanding the geometric orientation and intermolecular forces present in each isomer, as well as the energy barriers involved during the guest-cage binding and release process has vast implications. In order to use hydrocarbons as molecular separation tools instead of as a source for GHG emissions, a thorough understanding of guest properties that facilitate the highest rate of transfer and thermodynamic stability will ensure effective applications of MOCs and promote a more sustainable environment.

Acknowledgements:

This paper has been written through the mentorship of Jiratheep Pruchyathamkorn, PhD candidate at Cambridge University. Jiratheep Pruchyathamkorn is currently conducting various experiments for his thesis in the use of metal organic cages for molecular separation and chemical and physical stimuli that can impact the rate of encapsulation and release of guest-molecules in these cages.

References:

1. "Azo group(s) in selected macrocyclic compounds - PMC - NCBI." PMC, 8 Jan. 2018, www.ncbi.nlm.nih.gov/pmc/articles/PMC5845695/.

2. Fernandez, Carlos, et al. "Structural Flexibility in Metal-Organic Cages." Frontiers in Chemistry, vol. 9, 2021, pp. 1-14, www.frontiersin.org/articles/10.3389/fchem.2021.706462.

3. Kumar, Suresh, et al. "Recent advances in photocatalysis for environmental applications." Academia.edu, 2023, pp. 1-22, www.academia.edu/en/42036042/Recent_advances_in_photocatalysis_for_environmental_applications.

4. Li, Jian-Rong, et al. "Metal-Organic Cages for Catalysis." Accounts of Chemical Research, vol. 54, no. 12, 2021, pp. 3175-3186, pubs.acs.org/doi/10.1021/acs.accounts.1c00317.

5. Li, Jian-Rong, et al. "Metal-Organic Cages for Gas Storage and Separation." Chemical Reviews, vol. 119, no. 16, 2019, pp. 9703-9830, pubs.acs.org/doi/10.1021/acs.chemrev.8b00603.

6. "Metal-Organic Cages for Biomedical Applications - ACS Publications." ACS Publications, 2022, pubs.acs.org/doi/10.1021/acs.accounts.1c00729.

7. "Metal-organic cages as a platform for drug delivery and biomedical applications - RSC Advances (RSC Publishing)." RSC Advances, 2023, pubs.rsc.org/en/content/articlelanding/2023/ra/d0ra10205e#!divAbstract.

8. "Photocatalysis in Water-Soluble Supramolecular Metal Organic Complex - PMC - NCBI." PMC, 12 May 2023, www.ncbi.nlm.nih.gov/pmc/articles/PMC10221110/.

9. "Recent Advances of Photocatalytic Application in Water Treatment: A Review." PMC, vol. 20, no. 7, 2021, pp. 1-17, www.ncbi.nlm.nih.gov/pmc/articles/PMC8308214/.

10. "Recent developments in heterogeneous photocatalytic water treatment using visible light-responsive photocatalysts: a review - RSC Publishing." RSC Publishing, 2015, pubs.rsc.org/en/content/articlelanding/2015/ra/c4ra13734e.

11. "Structural Flexibility in Metal-Organic Cages - Frontiers." Frontiers, 2 Jun. 2021, www.frontiersin.org/articles/10.3389/fchem.2021.706462.

12. "Visible-Light Photoredox Catalysis in Water." PMC, vol. 21, no. 6, 2022, pp. 1-17, www.ncbi.nlm.nih.gov/pmc/articles/PMC10204095/.